

# Using Genetic Data to Build Intuition about Population History

Alan R. Rogers

January 11, 2022

## Abstract

Genetic data are now routinely used to study the history of population size, subdivision, and gene flow. A variety of formal statistical methods is available for testing hypotheses and fitting models to data. Yet it is often unclear which hypotheses are worth testing, which models worth fitting. There is a need for less formal methods that can be used in exploratory analysis of genetic data. One approach to this problem uses *nucleotide site patterns*, which provide a simple summary of the pattern in genetic data. This article shows how to use them in exploratory data analysis.

## 1 Nucleotide site patterns

Nucleotide site patterns are often used in computer programs designed to infer population history from genetic data [9–11, 13]. This article however is not concerned with computer programs. The goal here is to see what can be learned about population history simply by looking at the data. This introductory section will introduce site patterns and explain how they relate to history.

The left panel of Fig. 1 shows the relationship between three populations. I use capital letters to refer to populations:  $X$  is African,  $Y$  is Eurasian, and  $N$  is Neanderthal. Later on we will encounter  $D$ , which refers to Denisovans, an archaic population related to Neanderthals [8]. Combinations of letters refer to ancestral populations:  $XY$  is ancestral to  $X$  and  $Y$ ,  $XYN$  is ancestral to  $XY$  and  $N$ , and so on. The right panel of Fig. 1 shows the gene genealogy of a tiny sample consisting of three random nucleotides, one from  $X$ , one from  $Y$ , and one from  $N$ . All three are drawn from the same position within the genome. In practice we work with larger samples, involving multiple individuals and millions of nucleotide sites, but this tiny sample makes the principles easier to explain. I will call such samples “haploid,” because the sample from each population consists of a single nucleotide.

Haploid samples also provide a real advantage. When we trace larger samples backwards into the past, it occasionally happens that two lineages coalesce at their common ancestor to form a single ancestral lineage. This happens faster in small populations than in large ones, so the process is sensitive to population size. With a haploid sample, no coalescent events are possible until we reach an ancestral population that contains the ancestors of two or more of our modern samples. Consequently, recent changes in population size have no effect, and we need not incorporate them into our model. This makes it easier to study the distant past.

Figure 1 shows the gene genealogy of one hypothetical haploid sample, which is represented by the red and the gray lines. For this sample, the lineages from  $X$  and  $Y$  coalesce in population  $XY$ . Suppose that a mutation occurred somewhere on the red segment of the genealogy. A mutation generates a new allelic state, which we will call *derived* or *mutant* to distinguish it from the *ancestral* state that came before. If a mutation occurred on the red segment, we would observe the derived

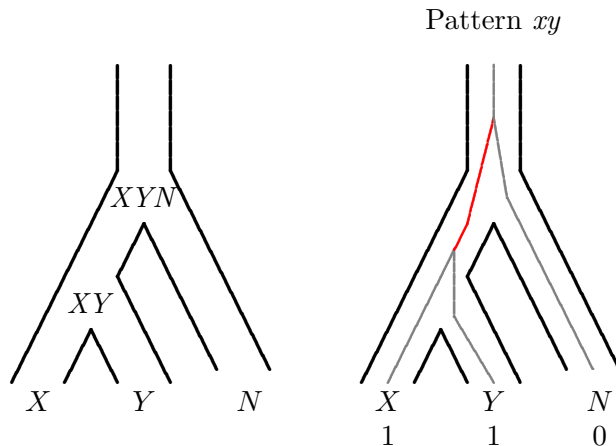


Figure 1: Population trees with notation (left) and an embedded gene genealogy (right). Population  $XY$  is ancestral to  $X$  and  $Y$ , and  $XYN$  is ancestral to  $XY$  and  $N$ . At the bottom of the right panel, “0” indicates the ancestral allele and “1” the derived (or mutant) allele. A mutation on the solid red segment would generate the  $xy$  site pattern. In this example, the closest relatives ( $X$  and  $Y$ ) uniquely share the derived allele.

allele in the samples from  $X$  and  $Y$  and the ancestral allele in that from  $N$ . I will call this outcome the “ $xy$  site pattern,” using lower case to distinguish site patterns from populations.

Before we can recognize site patterns in the data, we must first determine which allele is ancestral and which is derived. Figure 2 shows how this is done.

## 2 Data

Figure 3 shows site pattern frequencies of two modern human populations ( $X$ , Africa, and  $Y$ , Europe), and two archaic ones ( $N$ , Neanderthal, and  $D$ , Denisovan). In these data, the horizontal axis shows the relative frequency of each site pattern among the nucleotide sites in the genome, after excluding sites that fail quality control criteria, or for which the ancestral and derived alleles cannot be identified. The frequencies are plotted as open circles. Within each circle, the thing that looks like a dot is actually a horizontal line representing the 95% confidence interval. These intervals are very narrow, because these frequencies are estimated with high precision. This precision is possible because there is so much data in the nuclear genome.

Some of the pattern in these data is obvious. There are a lot of singletons ( $x$ ,  $y$ ,  $n$ , and  $d$ ), and two of the doubletons ( $xy$  and  $nd$ ) are more common than the others. Of the two common doubletons,  $xy$  is more common than  $nd$ . Other parts of the pattern are subtle: the less-common doubletons are similar in frequency, but  $yn$  is a little more common, and this difference is larger than the (barely-perceptible) confidence intervals.

To interpret these patterns, the trick is to reason as we did in Fig. 1 above. There, a mutation anywhere on the red segment of the gene genealogy would generate the  $xy$  site pattern. Anything that tended to lengthen this segment would inflate the frequency of this site pattern, because mutations are more likely to occur on long segments than on short ones. In the section that follows, we reason from population history to gene genealogies in order to understand the frequencies of site patterns.

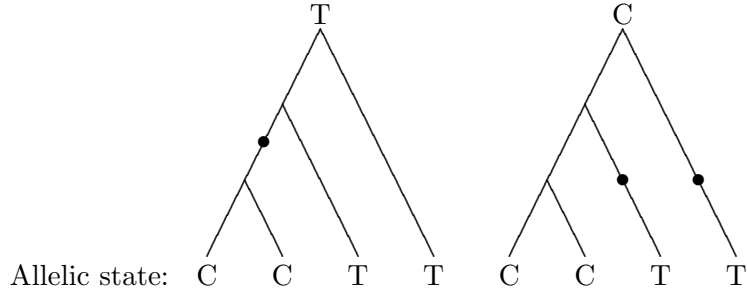


Figure 2: Calling ancestral and derived alleles. The solid lines represent a gene genealogy, with observed allelic states at the bottom. The letter at the top of each graph is an hypothesis about which allele is ancestral. The right-most sample in each graph is from an “outgroup”—a population that is distantly related to others. If  $C$  were ancestral, it would take two mutations (shown as bold dots) to produce the pattern in the data. Only one mutation is needed if  $T$  is ancestral. Because mutations are rare, a model that requires only one mutation is a better bet than one requiring two. We therefore infer that  $T$  is ancestral and  $C$  is derived.

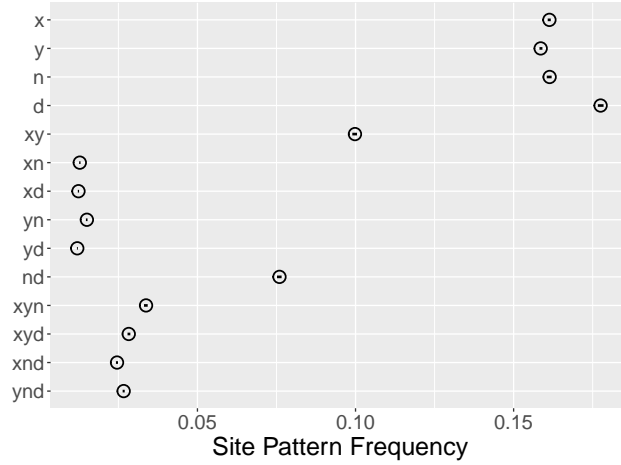


Figure 3: Observed site pattern frequencies. Horizontal axis shows the relative frequency of each site pattern in random samples consisting of a single haploid genome from each of four populations  $X$  (Africa),  $Y$  (Europe),  $N$  (Neanderthal), and  $D$  (Denisovan). Horizontal lines (which look like dots) are 95% confidence intervals estimated by a moving-blocks bootstrap [3]. Data: Simons Genome Diversity Project [4] and Max Planck Institute for Evolutionary Anthropology [6]. After Rogers et al. [13, Fig. S2].

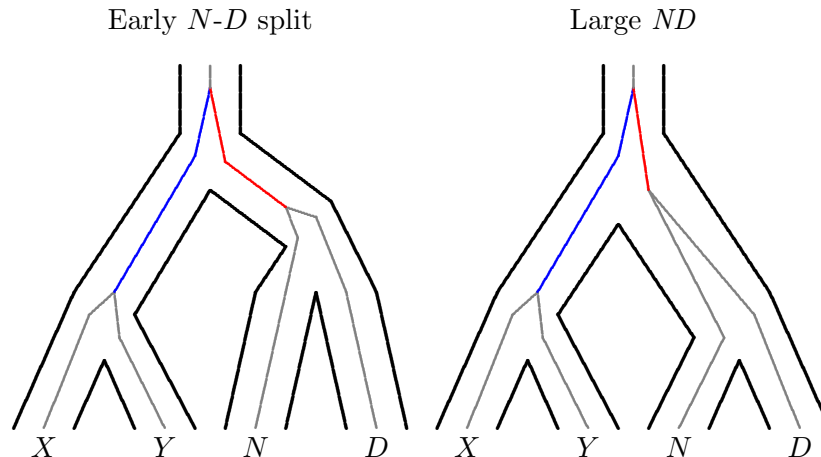


Figure 4: Gene genealogies that match the population tree.  $D$  is the Denisovan population. Other symbols are as in Fig. 1. The left and right panels illustrate different assumptions about the separation times of  $X$  and  $Y$  and of  $N$  and  $D$ , and about the effective sizes of populations  $XY$  (ancestral to  $X$  and  $Y$ ) and  $ND$  (ancestral to  $N$  and  $D$ ). The left panel assumes that the two separation times are unequal but the effective sizes of the two ancestral populations are the same. The right panel assumes the two separation times are the same but that the effective size of population  $ND$  is larger than that of  $XY$ .

### 3 Relating population history to site pattern frequencies

#### 3.1 When the gene genealogy agrees with the population tree

It is useful to start with a model that lacks gene flow. Such models often shed light on large-scale patterns, even if they miss the subtleties. Figure 4 shows two versions of such a model, each of which assumes that the two modern human populations ( $X$  and  $Y$ ) are closely related, and so are the two archaic ones ( $N$  and  $D$ ). Because there is no gene flow in these models, the network of populations has the shape of a tree. Within each population tree, I have drawn a gene genealogy, and in each genealogy the branching order is the same as that of the population tree. As we will see below, other branching orders also occur. However, this one is likely to be common, and if so it will explain the major features in the data.

In both sides of Fig. 4, a mutation on the blue segment would generate site pattern  $xy$ , whereas a mutation on the red segment would generate  $nd$ . These are the two common doubletons in Fig. 3. It makes sense that these patterns should be common, because  $X$  (Africa) and  $Y$  (Europe) are close relatives, as are  $N$  (Neanderthal) and  $D$  (Denisovan). Close relatives tend to share ancestors, and mutations in these shared ancestors inflate the frequencies of  $xy$  and  $nd$ . This is the verbal intuition behind the graphs in Fig. 4. The data imply that the two modern populations are close relatives as are the two archaic ones.

But why is  $xy$  more common than  $nd$ ? In Fig. 4, site pattern  $xy$  will arise only if a mutation occurs on the blue branch. This is more likely to happen if the blue branch is long than if it is short. Thus, the excess of  $xy$  over  $nd$  implies that, on average across the genome, the blue branch is longer than the red one. Why should these branches tend to differ in length?

The left and right panels of Fig. 4 illustrate two possible reasons. In the left panel, the separation between  $X$  and  $Y$  is more recent than that between  $N$  and  $D$ . For this reason,  $X$  and  $Y$  share a longer history of common ancestry than do  $N$  and  $D$ . Consequently, the blue branch is longer than the red one, and site pattern  $xy$  is more common than  $nd$ , just as we see in the data.

This is reassuring and probably also correct, but I have smuggled in a hidden assumption. As we trace the lineages from  $X$  and from  $Y$  backwards in time, they eventually arrive in population  $XY$ . Similarly, the lineages from  $N$  and  $D$  arrive in population  $ND$ , which is ancestral to  $N$  and  $D$ . In either case, as we trace the two lineages farther back in time, they eventually coalesce into a single parental lineage. In the previous paragraph, I assumed that this process takes the same length of time within populations  $XY$  and  $ND$ . This is not necessarily so.

Gene genealogies tend to be deeper in large populations than in small ones. Why? Because two random individuals are more likely to be close relatives in a small population. Close relatives are connected by short genealogies and distant relatives by deep ones. In the right panel of Fig. 4, population  $ND$  is much larger than  $XY$ , and it takes a long time for the  $N$  and  $D$  lineages to coalesce after they arrive in  $ND$ . In other words, they are connected by a deep genealogy. For this reason, the red branch is much shorter than the blue one. This is a second hypothesis that might explain the excess of  $xy$  over  $nd$  in the data.

It is not easy to choose between these alternatives, and this difficulty plagues formal statistical methods as well as the exploratory ones discussed here. In spite of this difficulty, we do have estimates, and these indicate that Neanderthals and Denisovans separated much earlier than did Africans and Europeans [8]. Furthermore, my colleagues and I have estimated that the population ancestral to Neanderthals and Denisovans was very small [11, 13]. Thus, neither of the assumptions made in the right panel of Fig. 4 is likely to be correct. The excess of  $xy$  over  $nd$  probably reflects a recent separation of  $X$  and  $Y$  rather than large size in population  $ND$ .

### 3.2 When the gene genealogy disagrees

Having explained several large-scale features in the data, let us focus now on a finer scale. It will be useful for a little longer to ignore the effect of gene flow. This will provide a base line against which effects of gene flow will become visible.

In this section, we concentrate on counterintuitive sites patterns—ones in which the derived allele is shared not by samples from closely-related populations, but by distant relatives. Consider for example the two histories shown in Fig. 5. In these examples, the lineages sampled in  $X$  and  $Y$  happen—just by chance—not to coalesce in population  $XY$ . They persist (going backwards in time) as distinct lineages throughout this segment of population history until they reach population  $XYN$  and are joined by the lineage sampled from  $N$ . At this point, we have three lineages within the larger population. I will assume that this population is not geographically subdivided. In this case, the three lineages are equally likely to coalesce in any order: either  $((X, Y), N)$ ,  $((X, N), Y)$ , or  $(X, (Y, N))$ . The two counterintuitive orders, which are illustrated in Fig. 5, generate site patterns  $xn$  and  $yn$ . The process that leads to these counterintuitive patterns is called *incomplete lineage sorting* [5].

Incomplete lineage sorting generates site patterns  $xy$ ,  $xn$ , and  $yn$  with equal frequency. However,  $xy$  is also generated by coalescent events within population  $XY$ , as illustrated in Fig. 1. Thus, in the absence of admixture, we expect  $xn$  and  $yn$  to be equally common, but neither of these should be as common as  $xy$ .

Returning now to the data in Fig. 3, note that  $xd$  is about equal in frequency to  $yd$ . These are counterintuitive site patterns in which the derived allele is shared by samples from distantly-related populations. If these site patterns were produced by incomplete lineage sorting, they should be equal in frequency, as indeed they seem to be.

On the other hand, the frequencies of  $yn$  and  $xn$  are not equal. Although the difference is not large in absolute terms, it is (as noted above) much larger than the confidence intervals. To understand what this might mean, we need to discuss the effect of gene flow between populations.

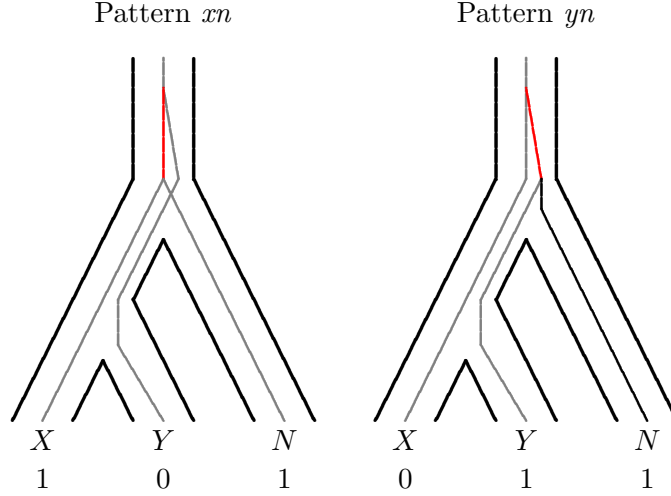


Figure 5: Incomplete lineage sorting: distant relatives may share derived allele. Absent gene flow, these site patterns should be equally frequent.

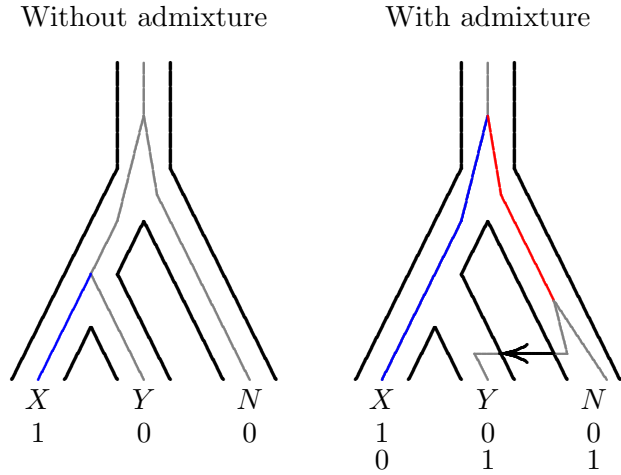


Figure 6: Neanderthal admixture into  $Y$  inflates the  $x$  and  $yn$  site patterns. Blue segment generates the  $x$  site pattern, red branch the  $yn$  site pattern.

### 3.3 The effect of gene flow

Figure 6 shows the result of gene flow from the Neanderthal population ( $N$ ) into the Eurasian one ( $Y$ ). This form of gene flow inflates the frequencies of the  $x$  and  $yn$  site patterns. In the figure, the blue branch is longer on the right than on the left, and this increases the frequency of  $x$ . The red branch on the right provides a mechanism (in addition to incomplete lineage sorting) that can generate  $yn$ . Both patterns can arise without gene flow, but they are more common when Neanderthals contribute DNA to Europeans.

These effects are not likely to be large. If only a small fraction of the lineages in  $Y$  derive via gene flow from  $N$ , then the histories of most nucleotide sites will be as described in Figs. 1, 4, and 5. In a complete genome from  $Y$ , only a small fraction of the nucleotide sites will derive from  $N$ . Consequently, the frequencies of site patterns  $yn$  and  $x$  will be inflated only slightly.

This is exactly the pattern seen in Fig. 3:  $yn$  is more common than  $xn$ , and  $x$  is more common than  $y$ . Although neither effect is large, both are larger than the confidence intervals. This pattern

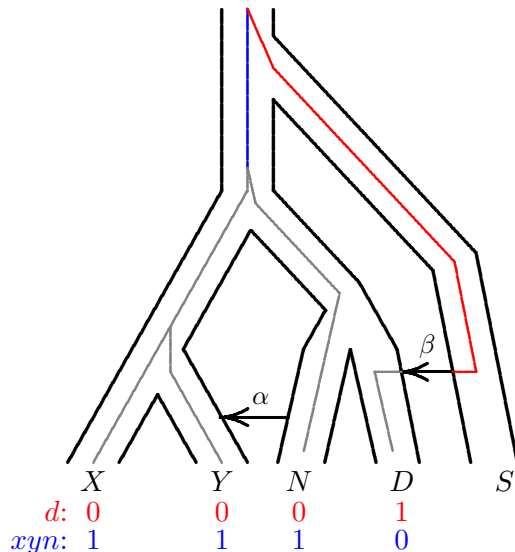


Figure 7: A population network including two episodes of gene flow, with an embedded gene genealogy. Upper case letters ( $X$ ,  $Y$ ,  $N$ ,  $D$ , and  $S$ ) represent populations (Africa, Europe, Altai Neanderthal, Denisovan, and superarchaic). Greek letters label episodes of gene flow.  $d$  and  $xyn$  illustrate two nucleotide site patterns, in which 0 and 1 represent the ancestral and derived alleles. A mutation on the red branch would generate site pattern  $d$ . One on the blue branch would generate  $xyn$ . After Rogers et al. [13, Fig. 1].

is the signature of Neanderthal gene flow into Europeans [1].

Finally, note that the  $d$  site pattern is substantially more common than the other singletons. This suggests that the Denisovan fossil is younger than the Altai Neanderthal. However, a detailed analysis of this hypothesis [12] led to the absurd conclusion that the Denisovan fossil was only 4000 years old—a date that is tens of thousands of years too young. Something was clearly missing from our model. Several authors had suggested that Denisovans received gene flow from a “superarchaic” population, which was distantly related to all other humans, archaic as well as modern [2, 6, 7, 14, 15]. If this hypothesis were correct, what effect might this have on site pattern frequencies?

Figure 7 provides an answer. Mutations on the red branch in this figure would inflate the frequency of site pattern  $d$ . Mutations on the blue branch would inflate  $xyn$ . Refer back to Fig. 3 and you will see that not only is  $d$  more common than the other singletons,  $xyn$  is more common than the other tripletons. This is the signature of superarchaic admixture into Denisovans [13].

## 4 Conclusions

This article has tested no hypotheses. Neither has it used any formal method to fit models to data. Yet we have learned a lot simply by looking at the data—by using it to build intuition about what models to fit and what hypotheses to test. Our exploratory analysis suggests that (a) modern Europeans and Africans are closely related, (b) so were Neanderthals and Denisovans, (c) the separation between Europeans and Africans was more recent than that between Neanderthals and Denisovans, (d) Neanderthals contributed DNA to Europeans, and (d) superarchaics contributed DNA to Denisovans. None of these findings are new, but it is useful to see that they can all be inferred simply by looking at the data.

## Acknowledgements

I am grateful for comments from Elizabeth Cashdan, Touhid Islam, Jan Koči, and Daniel Tabin. This work was supported by NSF grant BCS 1945782.

## References

- [1] Richard E. Green, Johannes Krause, Adrian W. Briggs, Tomislav Maricic, Udo Stenzel, Martin Kircher, Nick Patterson, Heng Li, Weiwei Zhai, Markus Hsi-Yang Fritz, Nancy F. Hansen, Eric Y. Durand, Anna-Sapfo Malaspinas, Jeffrey D. Jensen, Tomas Marques-Bonet, Can Alkan, Kay Prüfer, Matthias Meyer, Hernán A. Burbano, Jeffrey M. Good, Rigo Schultz, Ayinuer Aximu-Petri, Anne Butthof, Barbara Höber, Barbara Höffner, Madlen Siegemund, Antje Weihmann, Chad Nusbaum, Eric S. Lander, Carsten Russ, Nathaniel Novod, Jason Affourtit, Michael Egholm, Christine Verna, Pavao Rudan, Dejana Brajkovic, Željko Kucan, Ivan Gušić, Vladimir B. Doronichev, Liubov V. Golovanova, Carles Lalueza-Fox, Marco de la Rasilla, Javier Fortea, Antonio Rosas, Ralf W. Schmitz, Philip L. F. Johnson, Evan E. Eichler, Daniel Falush, Ewan Birney, James C. Mullikin, Montgomery Slatkin, Rasmus Nielsen, Janet Kelso, Michael Lachmann, David Reich, and Svante Pääbo. A draft sequence of the Neandertal genome. *Science*, 328(5979):710–722, 2010.
- [2] Martin Kuhlwilm, Ilan Gronau, Melissa J. Hubisz, Cesare de Filippo, Javier Prado-Martinez, Martin Kircher, Qiaomei Fu, Hernán A. Burbano, Carles Lalueza-Fox, Marco de la Rasilla, Antonio Rosas, Pavao Rudan, Dejana Brajkovic, Željko Kucan, Ivan Gušić, Tomas Marques-Bonet, Aida M. Andrés, Bence Viola, Svante Pääbo, Matthias Meyer, Adam Siepel, and Sergi Castellano. Ancient gene flow from early modern humans into Eastern Neanderthals. *Nature*, 530(7591):429–433, Feb 2016. ISSN 1476-4687.
- [3] Regina Y. Liu and Kesar Singh. Moving blocks jackknife and bootstrap capture weak dependence. In Raoul LePage and Lynne Billard, editors, *Exploring the “Limits” of the Bootstrap*, pages 225–248. Wiley, New York, 1992.
- [4] Swapan Mallick, Heng Li, Mark Lipson, Iain Mathieson, Melissa Gymrek, Fernando Racimo, Mengyao Zhao, Niru Chennagiri, Susanne Nordenfelt, Arti Tandon, Pontus Skoglund, Iosif Lazaridis, Sriram Sankararaman, Qiaomei Fu, Nadin Rohland, Gabriel Renaud, Yaniv Erlich, Thomas Willems, Carla Gallo, Jeffrey P. Spence, Yun S. Song, Giovanni Poletti, Francois Balloux, George van Driem, Peter de Knijff, Irene Gallego Romero, Aashish R. Jha, Doron M. Behar, Claudio M. Bravi, Cristian Capelli, Tor Hervig, Andres Moreno-Estrada, Olga L. Posukh, Elena Balanovska, Oleg Balanovsky, Sena Karachanak-Yankova, Hovhannes Sahakyan, Draga Toncheva, Levon Yepiskoposyan, Chris Tyler-Smith, Yali Xue, M. Syafiq Abdullah, Andres Ruiz-Linares, Cynthia M. Beall, Anna Di Rienzo, Choongwon Jeong, Elena B. Starikovskaya, Ene Metspalu, Jüri Parik, Richard Villems, Brenna M. Henn, Ugur Hodoglugil, Robert Mahley, Antti Sajantila, George Stamatoyannopoulos, Joseph T. S. Wee, Rita Khusainova, Elza Khusnutdinova, Sergey Litvinov, George Ayodo, David Comas, Michael F. Hammer, Toomas Kivisild, William Klitz, Cheryl A. Winkler, Damian Labuda, Michael Bamshad, Lynn B. Jorde, Sarah A. Tishkoff, W. Scott Watkins, Mait Metspalu, Stanislav Dryomov, Rem Sukernik, Lalji Singh, Kumarasamy Thangaraj, Svante Pääbo, Janet Kelso, Nick Patterson, and David Reich. The Simons Genome Diversity Project: 300 genomes from 142 diverse populations. *Nature*, 538:201–206, 2016. ISSN 1476-4687.



- [5] Pekka Pamilo and Masatoshi Nei. Relationships between gene trees and species trees. *Molecular Biology and Evolution*, 5(5):568–583, 1988.
- [6] Kay Prüfer, Cesare de Filippo, Steffi Grote, Fabrizio Mafessoni, Petra Korlević, Mateja Hladinjak, Benjamin Vernot, Laurits Skov, Pingsun Hsieh, Stéphane Peyrégne, David Reher, Charlotte Hopfe, Sarah Nagel, Tomislav Maricic, Qiaomei Fu, Christoph Theunert, Rebekah Rogers, Pontus Skoglund, Manjusha Chintalapati, Michael Dannemann, Bradley J. Nelson, Felix M. Key, Pavao Rudan, Željko Kućan, Ivan Gušić, Liubov V. Golovanova, Vladimir B. Doronichev, Nick Patterson, David Reich, Evan E. Eichler, Montgomery Slatkin, Mikkel H. Schierup, Aida Andrés, Janet Kelso, Matthias Meyer, and Svante Pääbo. A high-coverage Neandertal genome from Vindija Cave in Croatia. *Science*, 358(6363):655–658, 2017.
- [7] Kay Prüfer, Fernando Racimo, Nick Patterson, Flora Jay, Sriram Sankararaman, Susanna Sawyer, Anja Heinze, Gabriel Renaud, Peter H Sudmant, Cesare de Filippo, Heng Li, Swapan Mallick, Michael Dannemann, Qiaomei Fu, Martin Kircher, Martin Kuhlwilm, Michael Lachmann, Matthias Meyer, Matthias Ongyerth, Michael Siebauer, Christoph Theunert, Arti Tandon, Priya Moorjani, Joseph Pickrell, James C. Mullikin, Samuel H. Vohr, Richard E. Green, Ines Hellmann, Philip L. F. Johnson, Hélène Blanche, Howard Cann, Jacob O. Kitzman, Jay Shendure, Evan E. Eichler, Ed S. Lein, Trygve E. Bakken, Liubov V. Golovanova, Vladimir B. Doronichev, Michael V. Shunkov, Anatoli P. Derevianko, Bence Viola, Montgomery Slatkin, David Reich, Janet Kelso, and Svante Pääbo. The complete genome sequence of a Neanderthal from the Altai Mountains. *Nature*, 505(7481):43–49, 2014.
- [8] D. Reich, R. E. Green, M. Kircher, J. Krause, N. Patterson, E. Y. Durand, B. Viola, A. W. Briggs, U. Stenzel, P. L. F. Johnson, et al. Genetic history of an archaic hominin group from Denisova Cave in Siberia. *Nature*, 468(7327):1053–1060, 2010.
- [9] Alan R. Rogers. Legofit: Estimating population history from genetic data. *BMC Bioinformatics*, 20:526, 2019.
- [10] Alan R. Rogers. An efficient algorithm for estimating population history from genetic data. *bioRxiv*, 427922, 2021. Version 5 of this preprint has been peer-reviewed and recommended by *Peer Community In Mathematical and Computational Biology* (<https://doi.org/10.24072/pci.mcb.100003>).
- [11] Alan R. Rogers, Ryan J. Bohlender, and Chad D. Huff. Early history of Neanderthals and Denisovans. *Proceedings of the National Academy of Sciences, USA*, 114(37):9859–9863, 2017.
- [12] Alan R. Rogers, Ryan J. Bohlender, and Chad D. Huff. Reply to Mafessoni and Prüfer: Inferences with and without singleton site patterns. *Proceedings of the National Academy of Sciences, USA*, 114(48):E10258–E10260, 2017.
- [13] Alan R. Rogers, Nathan S. Harris, and Alan A. Achenbach. Neanderthal-Denisovan ancestors interbred with a distantly-related hominin. *Science Advances*, 6(8):eaay5483, 2020.
- [14] P. J. Waddell. Happy New Year *Homo erectus*? More Evidence for Interbreeding with Archaics Predating the Modern Human/Neanderthal Split. *ArXiv*, 1312.7749, December 2013.
- [15] Peter J Waddell, Jorge Ramos, and Xi Tan. *Homo denisova*, correspondence spectral analysis, finite sites reticulate hierarchical coalescent models and the Ron Jeremy hypothesis. *ArXiv*, 1112.6424, 2011.